

Momentum-resolved tunneling between a Luttinger liquid and a two-dimensional electron gas

S. A. Grigera and A. J. Schofield

School of Physics and Astronomy, University of Birmingham, Birmingham B15 2TT, United Kingdom

S. Rabello and Q. Si

Department of Physics, Rice University, Houston, Texas 77251-1892, USA

(Received 28 November 2003; revised manuscript received 25 March 2004; published 18 June 2004)

We consider momentum resolved tunneling between a Luttinger liquid and a two-dimensional electron gas as a function of transverse magnetic field. We include the effects of an anomalous exponent and Zeeman splitting on both the Luttinger liquid and the two-dimensional electron gas. We show that there are six dispersing features that should be observed in magneto-tunneling, in contrast with the four features that would be seen in a noninteracting one-dimensional electron gas. The strength of these features varies with the anomalous exponent, being most pronounced when $\gamma_\rho=0$. We argue that this measurement provides an important experimental signature of spin-charge separation.

DOI: 10.1103/PhysRevB.69.245109

PACS number(s): 71.10.Pm, 72.20.-i, 73.40.Gk

I. INTRODUCTION

Haldane's Luttinger-liquid hypothesis¹—that all one-dimensional (1D) metals are adiabatically continuous with the Tomonaga-Luttinger model^{2,3}—has underpinned our current understanding of the metallic state in one dimension. The low-energy properties of the metal are characterized by separate spin and charge velocities (v_σ and v_ρ , respectively) and, at most, two further anomalous exponents (γ_σ and γ_ρ). The low-energy excitations are completely different from those of the noninteracting electron gas. The one-dimensional metal is described in terms of spinons and holons rather than quasielectronlike excitations. As a result the low energy spectrum has no overlap with the corresponding noninteracting one and the metal is therefore a non-Fermi liquid.⁴

Although much is known theoretically about the properties of a Luttinger liquid (see, for example, Voit in Ref. 5), experimental verification of these ideas is on-going. A wide variety of measurements have been performed and interpreted within the Luttinger-liquid framework. These include work on the quasi-1D organics, inorganic charge-density wave materials, semiconductor quantum wires, and edge states in the fractional quantum Hall regime.^{6,7} However, most of these experiments have focused on identifying the anomalous exponents. Experiments which directly probe the separation of charge and spin in one dimension have proved to be more challenging. Arguably the most convincing measurements have been those of angle-resolved photoemission in metals⁸ and insulators.^{9,10} Nevertheless, there remains a need for a low-energy probe of the excitation spectrum of the Luttinger liquid.

In a recent paper,¹¹ Altland *et al.* proposed a spectroscopy of the Luttinger liquid state using magneto-tunneling. They showed how the tunneling conductance between a quasi-1D metal and a two-dimensional electron gas (the spectrometer) responds to a transverse magnetic field and allows features associated with the spinon and holon dispersion to be resolved. This momentum-conserving tunneling spectroscopy then provides a method of determining the low energy spec-

trum and identifying features associated with separate spin and charge excitations. In that paper, the authors considered, for simplicity, the special case where the anomalous exponents γ_ρ and γ_σ were both equal to 0. They also ignored the effect of the magnetic field on the spectral functions. The magnetic field was assumed to simply tune the relative momentum of the tunneling electron as it moves between the one-dimensional metal and the two-dimensional electron gas. This same tuning can also be achieved by changing the carrier density (and hence k_F) in either the wire or the two-dimensional electron gas. Experimentally, using a transverse magnetic field is likely to be by far the easiest way of tuning the intrachain momentum. The work of Altland *et al.* raised two further interesting questions that we will address here. First, how sensitive are the tunneling results to the value of the anomalous exponent? Perhaps more importantly, would the Zeeman splitting of Fermi-liquid quasiparticles give rise to two features and thereby mimic the spin-charge separation that the experiment was supposed to resolve?

In this paper we revisit the idea of momentum-dependent tunneling and solve for the tunneling conductance for arbitrary anomalous exponent γ_ρ . (The other exponent, γ_σ is equal to 0 in any rotationally symmetric system.) Recently two of the present authors¹² have also calculated the change in the Luttinger liquid spectral function due to a magnetic field. Using this result, we have now computed the tunneling conductance beyond the restrictions of Ref. 11. We find that the signature of magneto-tunneling into a Luttinger liquid is radically different from that in a noninteracting one-dimensional metal and the magnetic field reinforces this difference. The dispersion of spinons and holons may be separately identified from sharp features in the tunneling conductance. However, these features become less singular as the anomalous exponent varies away from zero.

The outline of the paper is as follows. We begin by establishing the formalism for magneto-tunneling when momentum parallel to the wire is conserved. We then introduce the spectral functions for arbitrary γ_ρ but initially ignore any change induced by the magnetic field. Next, we show how the magnetic field can straightforwardly be taken into ac-

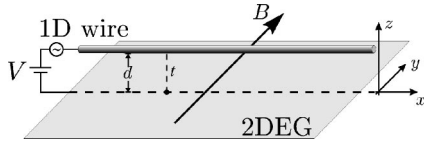


FIG. 1. Schematic representation of the tunneling geometry and field orientation for the magneto-tunneling experiment.

count within this formalism and we compute the tunneling conductance. Finally we discuss current attempts to perform this magneto-tunneling spectroscopy.

II. OVERVIEW

One of the advantages of this type of spectroscopy of correlated metals is that the theoretical interpretation of the experiment is extremely straightforward. We can therefore sketch our main findings before detailing more formally how they arise. The tunneling current between two metals is determined by the rate at which real physical electrons can hop between them. Since each metal is, in general, a complex interacting system, the physical electron is not an eigenstate of either metal. Thus the hopping rate is determined not just by the coupling between the two metals but by the overlap between a physical electron and the underlying eigenstates of the metallic state. The probability that a physical electron has a given energy and momentum in the metallic state is characterized by the spectral function—which contains all the information about this overlap. In the geometry considered in this paper, the tunneling electron moves through a finite voltage and transverse to an applied magnetic field (see Fig. 1). Thus the electron changes its energy (by eV) and also its momentum (by $\hbar q_B$ to be defined later) along the direction of the interface due to the Lorentz force acting on it during the tunneling process. The crucial assumption that we make in this paper is that the tunneling barrier is smooth so that momentum parallel to the 1D wire is conserved (up to this change due to the Lorentz force).

So, in summary, the tunneling current is determined by the joint probability that an electron with spin σ may be found on one side of the tunnel barrier with momentum k_x and energy ω and that there is an empty electron state with spin σ and with momentum $k_x + q_B$ and energy $\omega + eV$ on the other side of the barrier. This is then integrated over all k_x and ω to get the final current. However, what makes this measurement potentially useful is that in many interacting systems these probabilities (or spectral functions) contain well-defined features that in turn relate to the true eigenstates of the interacting system.

In this paper we consider there to be a Luttinger liquid on one side of the tunnel barrier. In a Luttinger liquid we know theoretically that there should be features in the electron spectral function related to the underlying excitations: spinons and holons. The dispersion of the spinons and holons can be seen in Fig. 2(a) as *two* lines of singularities of the spectral function in the ω, q plane. We assume that there is a two-dimensional Fermi liquid on the other side of the tunnel barrier. In a Fermi liquid there are electronlike quasiparticles

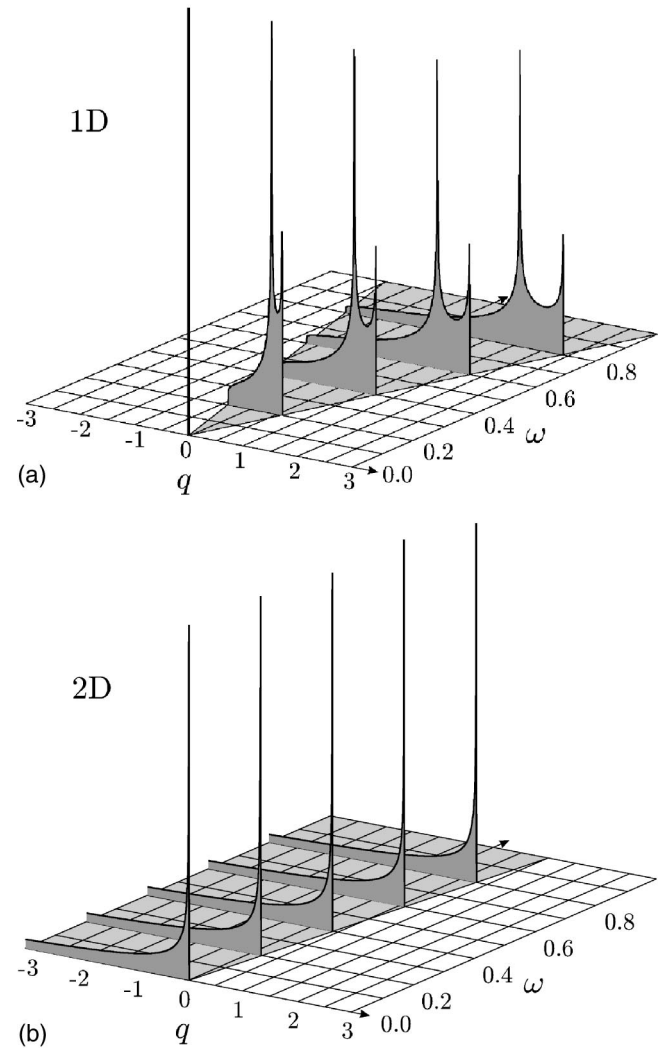


FIG. 2. (a) The electron spectral function in a Luttinger liquid for $\omega \geq 0$ and $\gamma_0 = 0.05$. The two dispersing singular features reflect the spinon and holon excitations. (b) The electron spectral function for a two-dimensional Fermi liquid integrated over k_y (perpendicular to the 1D wire). The single singular feature identifies the dispersion of the electronlike quasiparticle.

which are reflected in the spectral function as a *single* line of singularities in the ω, q plane [see Fig. 2(b)].

It is this profound difference in the nature of the excitations of a Luttinger liquid compared to a Fermi liquid that the magneto-tunneling experiment is designed to expose. Essentially the measurement measures the relative dispersion of the singular features in the 1D and 2D spectral functions as follows. The tunnel current is given by the integrated product of the two spectral functions of Fig. 2 with the magnetic field giving a relative offset along the q direction. Figure 3 shows that this product (and hence the current) divides into four distinct regions (a) to (d) depending on this magnetic field dependent offset and the dispersion of the singular features in the spectral functions. Thus the tunneling conductance shows three abrupt features separating the four regions as a function of applied magnetic field. These features can be seen in Fig. 4. Finally when one includes the Zeeman splitting there are separate tunneling processes for up- and down-

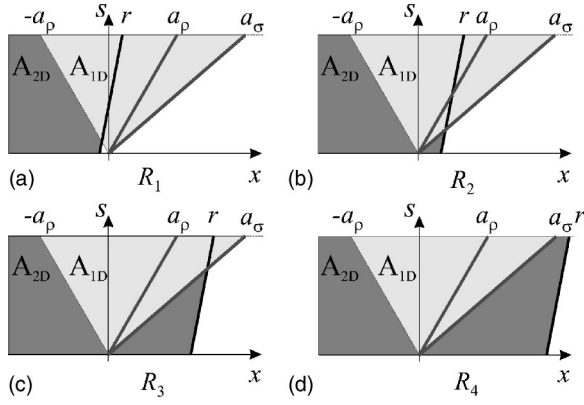


FIG. 3. The tunnel current is determined by the product of the spectral functions of Figs. 2(a) and 2(b) offset in momentum by q_B —an amount proportional to the transverse magnetic field. As the field is increased the region of overlap goes through four stages (a) to (d) labeled R_1 to R_4 in the text. The light dark and shaded areas represent, respectively, the areas where the one-dimensional and two-dimensional spectral functions have a finite nonzero value; the thick lines represent the lines of singularities.

spin electrons and the three abrupt features each split in two giving a total of six features in the conductance. This is shown in Fig. 5. The dispersion of these features as the magnetic field and applied voltage is changed also allows us to determine the relative velocity of the spinon and holon is shown in Fig. 6. In the absence of spin-charge separation there would be only one dispersing singularity in the 1D spectral function leading to four features in the tunneling conductance as a function of field. This then is the essence of our results and in the rest of the paper we give a more precise derivation of them.

III. FORMALISM

We consider single-electron tunneling between a one-dimensional interacting electron metal, parallel to the x axis, and a two-dimensional electron gas in the xy plane separated from the 1D wire by a distance d along the z direction. A potential difference is applied between the wire and the two-dimensional electron gas and a magnetic field is applied in the plane of the two-dimensional electron gas but perpendicular to the wire (along the y direction). The geometry is shown schematically in Fig. 1. The appropriate formalism was first derived in the context of superconductivity.¹³ The Hamiltonian for the system may be written as

$$\hat{H} = \hat{H}_{1D}(B) + \hat{H}_{2D}(B) + \hat{H}_T. \quad (1)$$

The precise forms of the one-dimensional wire \hat{H}_{1D} and the two-dimensional electron gas \hat{H}_{2D} are not required for determining the universal tunneling properties. Instead we will identify the universal aspects of the electron spectral function in these two systems by assuming that the one-dimensional system forms a Luttinger liquid and the two-dimensional system is a Fermi liquid. Thus for \hat{H}_{1D} and \hat{H}_{2D} we will take the canonical forms from which the Luttinger

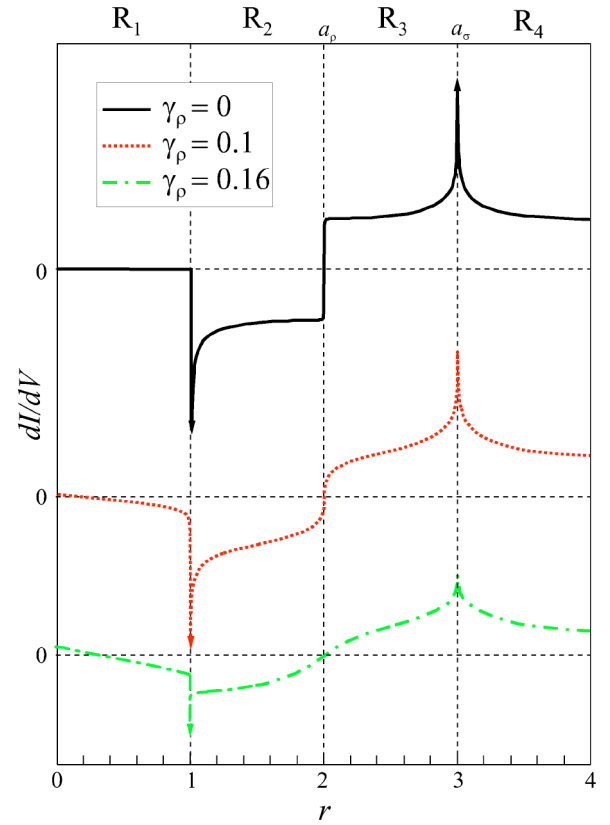


FIG. 4. (Color online) Differential tunneling conductance in the absence of Zeeman splitting shown as a function of dimensionless magnetic field $r = q_B v_F / eV$ for different values of the anomalous exponent γ_ρ and for dimensionless holon velocity $a_\rho = v_F / v_\rho = 2$ and spinon velocity, $a_\sigma = v_F / v_\sigma = 3$. The graphs have been shifted and rescaled for clarity. The arrows mark divergences. Notice how increasing the anomalous exponent from the noninteracting value of zero reduces the three features in the differential conductance.

liquid and Fermi liquid may respectively be adiabatically continued.

For the Fermi liquid we assume \hat{H}_{2D} is the Hamiltonian of a noninteracting gas of electrons with a free particle dispersion. This captures the electron quasiparticlelike character of the low lying excitations in a Fermi liquid up to an overall quasiparticle renormalization factor $z \leq 1$, which is simply a multiplicative factor in the tunneling current. It neglects the incoherent (nonuniversal) part of the spectral function and the ω^2 quasiparticle lifetime effects (we will only treat zero temperature). Similarly, \hat{H}_{1D} , is assumed to be a two-branch spin-full Luttinger model with inter- and intra-branch scattering.³ This model can be characterized by four parameters (spinon and holon velocities, and two anomalous exponents) which are the universal parameters of a general Luttinger liquid.¹

Equation (1) differs from the Hamiltonian considered in Ref. 11 since we have explicitly allowed a coupling of the magnetic field to the 1D and 2D electron systems. Since the field lies in the plane of the 2D electron gas however the coupling will be via the Zeeman interaction. The orbital part of the interaction with the magnetic field is included in the tunneling term

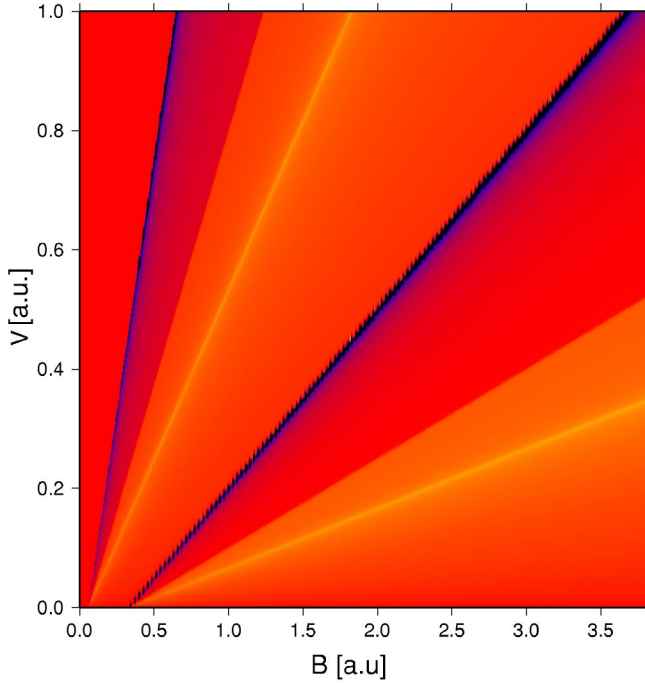


FIG. 6. (Color online) Contour plot of the differential conductance in the presence of a magnetic field as a function of B and V for a small anomalous exponent $\gamma_p=0.05$. Six dispersing features can be seen—indicative of spin-charge separation. The curves do not meet at $B=0$ because we do not assume the magnitude of k_F is the same in the 1D wire and the 2DEG. The differential conductance will be symmetric under $B \rightarrow -B$ as tunneling will then occur via the opposite branch of the Luttinger and 2DEG spectra.

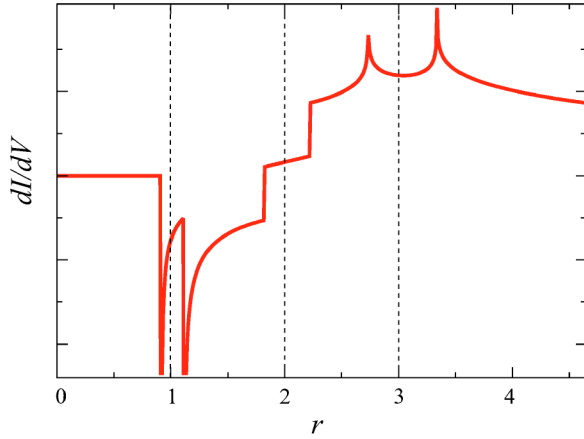


FIG. 5. Differential conductance including the effect of Zeeman coupling to a magnetic field as well as the orbital effect. The conductance is shown as a function of dimensionless magnetic field r for the noninteracting exponent $\gamma_p=0$ with dimensionless holon and spinon velocities $a_p=2$ and $a_s=3$. The Zeeman coupling (g factor) and the k_f are assumed to be identical in the 1D wire and the 2DEG ($\varsigma=\varsigma'=1$). The features in Fig. 4 appear to spin-split (to different degrees) by the Zeeman coupling.

$$\hat{H}_T = \int d\vec{r} dx t(x, \vec{r}) [e^{-iedB(x+r_x)/2} \hat{\Phi}_{2D, \sigma}^\dagger(\vec{r}) \hat{\Psi}_{1D, \sigma}(x) + \text{H.c.}]. \quad (2)$$

Here we have included the transverse magnetic field using the following gauge $\vec{A}=(0, 0, -Bx)$ and the usual Peierls coupling. The crucial assumption behind this method is that the tunneling amplitude $t(x, \vec{r})$ for an electron to move from position x in the 1D to position \vec{r} in the 2D gas is translationally invariant—i.e., that the tunnel barrier is smooth—and so may be written as $t(x-x_{2D}, y_{2D})$. We also assume that this single electron tunneling is weak (so as not to significantly disturb the excitation spectrum in the 1D and 2D systems) and is the only term coupling the systems together.

In momentum space then this coupling may be written as

$$\hat{H}_T = \sum_{\vec{k}} t_{\vec{k}} \hat{\phi}_{k_x - q_B/2, k_y, \sigma}^\dagger \hat{\psi}_{k_x + q_B/2, \sigma} + \text{H.c.}, \quad (3)$$

where $q_B = eBd + k_f^{2D} - k_f^{1D}$. Thus we see that momentum parallel to the 1D wire is conserved up to the change induced by moving the applied magnetic field. The applied field then tunes the tunneling momentum of the electron. Here $t_{\vec{k}}$ is the Fourier transform of the tunneling matrix element.

Given the tunneling Hamiltonian, it is then straightforward to determine the tunneling current to leading order in t . Note that our starting Hamiltonian neglects any interactions between the two-dimensional electron gas and the quantum wire—the only coupling is via single electron tunneling. Thus with this assumption there are no vertex corrections in the tunneling current and it can be written directly in terms of the single electron Greens function for the 2D electron gas and the quantum wire. The form for the current is most intuitively expressed in terms of the electron spectral functions for the 2D and 1D systems, respectively,

$$I(B, V) = \frac{e}{\pi} \int d\omega \sum_{\vec{k}} t_0^2 [f(\omega) - f(\omega - eV)] A_{1D}(k_x + q_B/2, \omega, B) A_{2D}(k_x - q_B/2, k_y, \omega - eV, B), \quad (4)$$

where f is the Fermi distribution function. The derivation is given, for example, in Mahan¹⁴ and Eq. (4) differs only from Eq. (9.3.11) in Ref. 14 in that we assume that tunneling is through a translationally invariant interface via nearest contact only so that $t(x-x_{2D}, y_{2D}) = t_0 \delta(x-x_{2D}) \delta(y_{2D})$. Thus we have momentum conservation along the direction of the wire up to any momentum change due to the Lorentz force from the transverse magnetic field. Explicitly we have, in the notation of Mahan¹⁴

$$|T_{\mathbf{k}, \mathbf{p}}|^2 = |t|^2 \delta(k_x - p_x + q_B). \quad (5)$$

It would be straightforward to relax the nearest contact assumption by introducing an additional “aperture function” which would need to be included in the momentum convolution.

IV. TUNNELING WITH GENERAL γ_ρ

We start by specifying the spectral functions used in the calculation of the current. For the two-dimensional system the spectral function $A_{2D,\eta}$ for energies close to the Fermi energy (and integrated over the momentum component transverse to the wire) is given by¹¹ (see Fig. 2)

$$A_{2D}(q, \omega) = \sqrt{2m} \frac{\Theta(\omega - qv_F)}{\sqrt{\omega - qv_F}}. \quad (6)$$

The spectral function of a Luttinger liquid with spin rotation-invariant interactions ($\gamma_\sigma=0$) is nontrivial (see Fig. 2), and a closed and tractable analytic expression is still lacking in the literature. However, we are concerned with universal features that may be seen in the tunneling current and these features will arise from the singularities in the spectral functions as they are convolved. Thus we only require the asymptotic behavior of the spectral function near these singularities and these are well characterized.^{5,15}

We can describe what is known about these singularities as follows. At very small q , the function looks very similar to a spinless fermion's function. As q is increased two peaks become apparent, a reflection of spin-charge separation, one at $v_\sigma q$ and another at $v_\rho q$, where v_ρ and v_σ are the velocities of charge and spin density waves, respectively. The exponent of the singularity at $v_\sigma q$ is $2\gamma_\rho - \frac{1}{2}$ and the corresponding one at $v_\rho q$ is $\gamma_\rho - \frac{1}{2}$. The function terminates at negative q at $-v_\rho q$ with a nonsingular exponent γ_ρ . The parameter γ_ρ , which characterizes the interactions between left and right movers is always positive. The case of noninteracting left and right branches, which was studied in Ref. 11, corresponds to the case $\gamma_\rho=0$. As γ_ρ increases, the power law divergences gradually weaken into cusp singularities, and the spectral weight, which for $\gamma_\rho=0$ is confined within $v_\sigma q$ and $v_\rho q$ is gradually transferred by the electronic correlations toward higher values of q and ω . The spectral function should also be invariant to the transformations ($p \rightarrow -p; q \rightarrow -q$) where $p = \pm$ labels left and right movers, and ($\omega \rightarrow -\omega; q \rightarrow -q$).

Since the spectral functions away from these singularities are likely to be nonuniversal, and in any case lead only to the background tunneling current, we can capture the universal physics by a function which has identical asymptotes to the same singularities. For $\omega > 0$, the case of our interest, a function that has the correct singularities and asymptotic behavior can be written as

$$A_{1D}(q, \omega) = \frac{W(q, \omega)\Theta(\omega - qv_\sigma)}{|\omega - v_\sigma q|^{1/2-2\gamma_\rho} |\omega - v_\rho q|^{1/2-\gamma_\rho}}$$

where

$$W(q, \omega) = \begin{cases} \Theta(qv_\rho - \omega) + \Theta(\omega - qv_\rho)c(\gamma_\rho) & \text{if } \gamma_\rho \neq 0 \\ \Theta(qv_\rho - \omega) & \text{if } \gamma_\rho = 0, \end{cases} \quad (7)$$

for $q > 0$ plus a nondivergent term for $q < 0$ and $\gamma_\rho \neq 0$ which is proportional to

$$\Theta(\omega + v_\rho q)c(\gamma_\rho)(\omega + v_\rho q)^{\gamma_\rho}. \quad (8)$$

This function is not normalizable for $\gamma \neq 0$. In our case the consequences of this are merely reduced to an undetermined constant that multiplies the conductivity for each γ_ρ . Note also that, although it is an approximation to replace the true spectral function of a Luttinger liquid by the asymptotic form of Eq. (7), we will correctly obtain the position and form of singularities in the tunneling current which are the main results of this paper. It is unlikely to capture smooth variations or the absolute magnitude of the tunneling current, but neither are these features expected to be universal. In this paper we will consider the case $v_F > v_\rho > v_\sigma$, but it should be noted that the results can be trivially extended to consider the other possible cases.

Substituting Eqs. (6) and (7) into Eq. (4) we find for the tunneling current at $T=0$

$$I(V, B) = \frac{4\sqrt{2}I_0(eV)^{1/2+3\gamma_\rho}}{\pi\sqrt{mv_F}} \sum_\alpha \int_{l_\alpha}^{u_\alpha} dx \int_{L_\alpha}^{U_\alpha} ds \\ \times \frac{a_\sigma^{1/2-2\gamma_\rho} a_\rho^{1/2-\gamma_\rho}}{|sa_\sigma - x|^{1/2-2\gamma_\rho} |sa_\rho - x|^{1/2-\gamma_\rho} |s - x + (r-1)|^{1/2}}, \quad (9)$$

where we have introduced the dimensionless parameters $r = q_B v_F / eV$, $a_\rho = v_F / v_\rho$, and $a_\sigma = v_F / v_\sigma$ and the dimensionless one-dimensional variables $x = qv_F / eV$ for the 1D wire wavevector and $s = \omega / eV$ for the frequency. $I_0 = e|t|^2 m / \pi$ is the natural unit for current in this problem. From this integral we identify four different regions with different qualitative behavior, R_j , $j=1, \dots, 4$, corresponding to different situations of overlap between the one- and two-dimensional spectral functions. Figure 3 is a schematic representation of the relative positioning between A_{1D} and A_{2D} in the four regions. In terms of the dimensionless parameters these are given by R_1 : $r < 1$; R_2 : $1 \leq r \leq a_\rho$; R_3 : $a_\rho \leq r < a_\sigma$; and R_4 : $r > a_\sigma$. In each region, and for practical reasons only, the calculation is in turn split into different integrals of the same integrand. Table I lists the upper and lower limits corresponding to each different region. Although the majority of these integrals cannot be integrated analytically, the asymptotic behavior in the different regions can be obtained by standard calculus procedures. The $q < 0$ nonsingular part of the spectral function for $\gamma \neq 0$ [Eq. (8)] only contributes a small featureless onset of conductivity at $r = -a_\rho$, and a background of finite conductivity noticeable only for small values of r and big values of γ_ρ .

Figure 4 shows the differential conductance $G = dI/dV$ as a function of the dimensionless parameter r at $T=0$. In the following we discuss the behavior of G in each regime.

R_1 .—For $r < 1$ and $\gamma_\rho \neq 0$ A_{2D} overlaps with the nondivergent part of A_{1D} , leading to a finite but nonsingular flow of current, with negative differential conductance. When r reaches the value of 1, the conductance diverges as $g \sim -(1-r)^{-1/2+3\gamma_\rho}$, where $g = G\sqrt{E_F}e^{1/2+3\gamma_\rho}V^{-1/2+3\gamma_\rho}/I_0$ is a dimensionless measure of the conductance. For $\gamma_\rho=0$ the two areas do not overlap, implying that the current vanishes.

R_2 .—For $r > 1$, the spectral functions for $\gamma_\rho=0$ start overlapping as well, and the conductance diverges as

TABLE I. Integration limits for Eq. (9) in the four different regions of spectral function overlap shown in Fig. 3.

Region	α	l_α	u_α	L_α	U_α
R_1	1	0	r	$x-(r-1)$	1
R_2	1	0	$r-1/a_\sigma-1$	sa_ρ	sa_σ
	2	$r-1/a_\sigma-1$	$r-1/a_\rho-1$	sa_ρ	$s+(r-1)$
	3	0	$r-1/a_\rho-1$	0	sa_ρ
	4	$r-1/a_\rho-1$	1	0	$s+(r-1)$
R_3	1	0	$r-1/a_\sigma-1$	sa_ρ	sa_σ
	2	$r-1/a_\sigma-1$	1	sa_ρ	$s+(r-1)$
	3	0	1	0	sa_ρ
R_4	1	0	1	sa_ρ	sa_σ
	2	0	1	0	sa_ρ

$g \sim -(r-1)^{-1/2+3\gamma_\rho}$. For finite γ_ρ , however, the cusp is also not symmetric (see Fig. 4) since the spectral weight of the singularity is different at either side of qv_ρ . The behavior of the conductance is unaltered up to the boundary to R_3 , where

$$g(a_\rho^+) - g(a_\rho^-) = \frac{a_\rho}{a_\rho - 1} \frac{a_\sigma^{1/2-2\gamma_\rho} a_\rho^{1/2-\gamma_\rho}}{(a_\sigma - a_\rho)^{1/2-2\gamma_\rho}} \lim_{r \rightarrow a_\rho} (r - a_\rho)^{\gamma_\rho}, \quad (10)$$

$a_\rho^\pm = a_\rho \pm \delta$, δ infinitesimal and positive. This implies that for $\gamma_\rho = 0$, the conductance exhibits a discontinuity Δ , the magnitude of which is

$$\Delta = \frac{a_\rho}{a_\rho - 1} \sqrt{\frac{a_\sigma a_\rho}{a_\sigma - a_\rho}}. \quad (11)$$

For every nonzero value of γ_ρ this step is rounded off (see Fig. 4) into a continuous function with a pronounced change at a_ρ , the change decreasing progressively as γ_ρ is increased.

R_3 .—In this region the differential conductance becomes positive. As r approaches the singularity line corresponding to a_σ , the boundary with R_4 , the conductance shows a pronounced increase. Again the case of $\gamma_\rho = 0$ is unusual, since the boundary between R_3 and R_4 shows a singularity, which is of logarithmic type

$$g(r, \gamma_\rho = 0) \rightarrow_{r \rightarrow a_\sigma} - \frac{a_\sigma}{a_\sigma - 1} \sqrt{\frac{a_\rho a_\sigma}{a_\sigma - a_\rho}} \frac{1}{\pi} \ln(a_\sigma - r). \quad (12)$$

On the other hand, for any nonzero γ_ρ , the behavior is found to be

$$g(r) \rightarrow_{r \rightarrow a_\sigma} - \frac{a_\sigma}{a_\sigma - 1} \frac{a_\rho^{1/2-\gamma_\rho} a_\sigma^{1/2-2\gamma_\rho}}{(a_\sigma - a_\rho)^{1/2-3\gamma_\rho}} \frac{1}{\pi} \lim_{r \rightarrow a_\sigma} {}_2F_1 \left[\begin{matrix} 1/2 \\ 1/2 + 2\gamma_\rho, 1/2 + \gamma_\rho, 1 + 2\gamma_\rho, \frac{a_\rho - r}{a_\rho - a_\sigma} \end{matrix} \right], \quad (13)$$

which is a nondivergent peak (see Fig. 4).

R_4 .—The boundary is symmetric in r around a_σ . The asymptotic behavior is $g \sim r^{-1/2}$ for all values of γ_ρ .

V. ADDING A ZEEMAN SPLITTING

In this section we consider the effects on the spectral functions of a Zeeman coupling to the magnetic field. Very recent work by two of the authors of this paper¹² has derived the spectral functions of a Luttinger liquid with a Zeeman term in the Hamiltonian.

$$A_{1D}(q, \omega, \mathbf{s}) = \frac{W(q, \omega) \Theta(\omega - qv_\sigma - \mathbf{s}B)}{|\omega - v_\sigma q - \mathbf{s}B|^{1/2-2\gamma_\rho} |\omega - v_\rho q - \mathbf{s}Bv_\rho/v_\sigma|^{1/2-\gamma_\rho}} \quad (14)$$

where

$$W(q, \omega) = \begin{cases} \Theta(qv_\rho - \mathbf{s}Bv_\rho/v_\sigma - \omega) + \Theta(\omega - qv_\rho - \mathbf{s}Bv_\rho/v_\sigma) c(\gamma_\rho) & \text{if } \gamma_\rho \neq 0 \\ \Theta(qv_\rho - \mathbf{s}Bv_\rho/v_\sigma - \omega) & \text{if } \gamma_\rho = 0, \end{cases} \quad (15)$$

where \mathbf{s} takes the value of the spin ($\pm 1/2$) times the Zeeman coupling factor. We have considered only positive q and ω , since as we discussed in the previous section, the contribution of $q < 0$ is merely to add a finite background of conduc-

tivity. (This background is very small for $\gamma_\rho \sim 0$.) Furthermore, we have seen that the region of interest, where the features in the spectral functions are easily distinguished in the differential conductivity, is restricted to small values of

the anomalous exponent (below $\gamma_\rho \approx 0.2$); for these values of γ_ρ the spectral weight outside the qv_ρ, qv_σ region is so small that all nondivergent contributions from A_{1D} outside this interval are negligible.

The effect of the magnetic field in the two-dimensional system is taken into account by writing the spectral function as

$$A_{2D}(q, \omega, s') = \frac{\sqrt{m} \Theta(\omega - qv_F - s'B)}{\sqrt{2} \sqrt{\omega - qv_F - s'B}}, \quad (16)$$

where s' is the equivalent of s for the two-dimensional system.

Since we can split the current into the separate contributions of the two possible values of the spin

$$I = I_\downarrow + I_\uparrow \quad (17)$$

the problem is reduced to the calculation of the integral

$$I_{\downarrow, \uparrow}(V, B) = \frac{4\sqrt{2}I_0(eV)^{1/2+3\gamma_\rho}}{\pi\sqrt{m}v_F} \int dq \int d\varepsilon [f(\varepsilon - eV) - f(\varepsilon)] A_{1D}(q, \omega, s) A_{2D}(q, \omega, s'). \quad (18)$$

We can make use of the results of the previous section and simplify the calculation considerably by defining the spin dependent variable $q' = q - sB/v_s$, and the spin dependent parameter

$$r_{\downarrow, \uparrow} = r \pm \frac{s'v_\sigma - sv_F}{v_\sigma} \frac{B}{eV}. \quad (19)$$

The general expressions for the current and the differential conductance then reduce to

$$I_Z = \frac{1}{2} [I(r_\uparrow) + I(r_\downarrow)], \quad (20)$$

$$g_Z = \frac{1}{2} [g(r_\uparrow) + g(r_\downarrow)], \quad (21)$$

where $I(r)$ and $g(r)$ are the functions for the current and the conductance derived in the previous section. Figure 5 shows the differential conductivity as a function of r for $\gamma_\rho = 0$, $a_\rho = 2$, $a_\sigma = 3$, $s = s' = 1$, and $k_f^{2D} = k_f^{1D}$. The different degree of field splitting of the different features in the conductivity can clearly be seen.

VI. CONCLUSIONS

Having calculated the generalized form of the magnetotunneling conductance we see that the key signature of the types of excitation in a Luttinger liquid is revealed in the appearance of six features which disperse with applied field. Loosely this may be viewed as the allowed transitions between spin-split spinon and holon excitations and the spin-split electron in the two-dimensional electron gas. However, this differs dramatically from the case of electronlike excitations in the one-dimensional metal which would display four features. So this directly addresses the issue as to whether

Zeeman splitting and spin-charge separation are distinguishable in this experiment—they are.

The effect of an anomalous exponent is more subtle. The original proposal of Ref. 11 took the case of $\gamma_\rho = 0$ for calculational simplicity. The more general treatment given here shows that this is, in fact, the most singular case and other values for the anomalous exponent leads to less pronounced effects. Nevertheless, if γ_ρ is not too far from zero, there will still be six clearly distinguishable features. In the Luttinger model, γ_ρ comes from interbranch processes, while spin-charge separation is due primarily to forward scattering intrabranch effects. Thus it is possible that spin-charge separation and an anomalous exponent not far from the noninteracting value of one could coexist in real quantum wires.

The role of the anomalous exponent in weakening the tunneling singularities has implications for other forms of momentum-resolved tunneling experiments. Recently Carpentier *et al.*¹⁶ have analyzed the tunneling conductance between two Luttinger liquids in a magnetic field (though without including the Zeeman effects as is done here). Again the tunneling current can be viewed as a convolution but now of two Luttinger liquid spectral functions. An anomalous exponent which differs from the noninteracting value will weaken the singularities in both functions in the convolution and will be doubly detrimental to features in the conductance. Thus we believe that using a two-dimensional Fermi liquid as the spectrometer, as described in this paper, optimizes the probability of seeing the dispersing features of the Luttinger liquid. This is because the Fermi liquid theory will always guarantee a square-root singularity in its spectral function (after integration over the transverse momentum) which is the best one can do.

The experimental challenges in carrying out this experiment should not be underestimated. We rely on a number of assumptions. The most obvious is that tunneling is occurring uniformly along the 1D to 2D interface rather than via pointlike tunneling. The test for whether an experiment is in this regime comes from the magnetic field dependence. With pointlike tunneling, one would expect only weak field dependence of the tunneling current since momentum would no longer be conserved along the wire. Experiments using molecular beam epitaxy grown interfaces have shown¹⁷ that the tunnel barriers can be sufficiently well controlled to preserve momentum conservation along the wire during tunneling, hence we believe that semiconductor fabricated quantum wire to 2D metal interfaces will be the most promising candidate.

The second assumption is that the two-dimensional system is a well-controlled Fermi liquid with a large electron weight in the quasiparticle $Z \sim 1$. This ensures that the overlap between the electron and the excitations in the 2D spectrometer are large. Again, estimates from semiconductor two-dimensional electron gases (2DEGs) suggest that this is not implausible.

Our final assumption is that the rate limiting step in the experiment is the tunneling process between the 1D and 2D systems. This requires a clean quantum wire with no impurities breaking the wire up into smaller pieces. Early results suggest that this may be causing problems in trying to imple-

ment this experiment in semiconductor devices.¹⁷ There the quantum wire is made by “pinching off” a channel in a two-dimensional electron gas with an applied gate voltage. This pushes the one-dimensional subbands through the chemical potential until only one remains active. Initial experimental results reveal magneto-tunneling occurring when multiple subbands are conducting but the wire becomes insulating in the last subband. This is presumably due to impurities blocking conduction (an interesting process in itself).¹⁸ Ultimately, we believe that this should be viewed as a challenge rather than a fundamental flaw in the experiment. However, it also suggests that we should look at alternative realizations of this experiment. One possibility is to use carbon nanotubes as quantum wires since these have already been used to demonstrate Luttinger liquidlike behavior¹⁹ via point tunneling. If a suitable interface could be found with a two-dimensional conventional metal this would be a good alternative candidate for the magneto-tunneling measurement.

Finally we should point out that, although we have used a magnetic field for tuning the relative momentum between the wire and spectrometer, this is not the only method. Using a semiconductor 2DEG one could back-gate the device and control the carrier concentration, and hence k_F , in the spectrometer. This gate voltage would then provide the momentum tuning via the difference in k_F between the wire and the 2DEG. Such a method could be used in cleaved edge overgrowth devices where the tunnel barrier to the quantum wire is in the plane of the 2DEG.²⁰ Using k_F to tune the momentum would, of course, mean there is no need to consider Zeeman coupling. However, the results may be complicated by any carrier concentration dependence of the 2DEG on its

Fermi liquid properties, or indeed on the parameters of the Luttinger liquid which may be renormalized via screening from the 2DEG.

To summarize, we have considered momentum-conserving tunneling between a Luttinger liquid and a two-dimensional conventional metal. We have shown how a transverse magnetic field can be used to tune the relative momentum of the tunneling electron. This then provides a direct measure of the spectral function of a Luttinger liquid via its convolution with that of a conventional Fermi liquid. The signatures of spin-charge separation are revealed as features in the tunneling conductance and we have shown they vary as a function of Zeeman splitting and anomalous exponent. The advantage of this experiment is that it can be performed with high resolution compared to other probes of the spectral function such as angle-resolved photoemission. Also the experiment has a very straightforward theoretical interpretation and hence, if successful, is an unambiguous detector of spin-charge separation. We have also discussed the prospects of performing such an experiment.

ACKNOWLEDGMENTS

The authors have benefited from useful discussions with T. S. Grigera, M. W. Long, and L. Macks and we thank A. P. Mackenzie for a critical reading of the manuscript. We are grateful for the financial support of the Leverhulme Trust, The Royal Society, and NATO Collaborative Research Grant No. 971072. Two of us (S.R. and Q.S.) have been supported in part by the Robert A. Welch Foundation, NSF Grant No. DMR-0090071, and TcSAM.

¹F. D. M. Haldane, *J. Phys. C* **14**, 2585 (1981).

²S. Tomonaga, *Prog. Theor. Phys.* **5**, 544 (1950).

³J. M. Luttinger, *J. Math. Phys.* **4**, 1154 (1963).

⁴A. J. Schofield, *Contemp. Phys.* **40**, 95 (1999).

⁵J. Voit, *Rep. Prog. Phys.* **58**, 977 (1995).

⁶A. M. Chang, L. N. Pfeiffer, and K. W. West, *Phys. Rev. Lett.* **77**, 2538 (1996).

⁷A. M. Chang, M. K. Wu, C. C. Chi, L. N. Pfeiffer, and K. W. West, *Phys. Rev. Lett.* **86**, 143 (2001).

⁸P. Segovia, D. Purdie, M. Hengsberger, and Y. Baer, *Nature (London)* **402**, 504 (1999).

⁹C. Kim, A. Y. Matsuura, Z. X. Shen, N. Motoyama, H. Eisaki, S. Uchida, T. Tohyama, and S. Maekawa, *Phys. Rev. Lett.* **77**, 4054 (1996).

¹⁰H. Fujisawa, T. Yokoya, T. Takahashi, S. Miyasaka, M. Kibune, and H. Takagi, *Phys. Rev. B* **59**, 7358 (1999).

¹¹A. Altland, C. H. W. Barnes, F. W. J. Hekking, and A. J.

Schofield, *Phys. Rev. Lett.* **83**, 1203 (1999); cond-mat/9907459.

¹²S. Rabello and Q. Si, cond-mat/0008065.

¹³J. R. Schrieffer, D. J. Scalapino, and J. W. Wilkins, *Phys. Rev. Lett.* **10**, 336 (1963).

¹⁴G. D. Mahan, *Many-Particle Physics*, 2nd ed. (Plenum Press, New York, 1990).

¹⁵V. Meden and K. Schönhammer, *Phys. Rev. B* **46**, 15753 (1992).

¹⁶D. Carpentier, C. Peca, and L. Balents, cond-mat/0103193.

¹⁷B. Kardynal, C. H. W. Barnes, E. H. Linfield, D. A. Ritchie, J. T. Nicholls, K. M. Brown, G. A. C. Jones, and M. Pepper, *Phys. Rev. B* **55**, R1966 (1997).

¹⁸C. L. Kane and M. P. A. Fisher, *Phys. Rev. B* **46**, 15233 (1992).

¹⁹M. Bockrath, D. H. Cobden, J. Lu, A. G. Rinzler, R. E. Smalley, L. Balents, and P. L. McEuen, *Nature (London)* **397**, 598 (1999).

²⁰R. de Picciotto, H. L. Stormer, A. Yacoby, L. N. Pfeiffer, K. W. Baldwin, and K. W. West, *Phys. Rev. Lett.* **85**, 1730 (2000).